



In Vivo Assessment of Drug Efficacy against Mycobacterium abscessus Using the Embryonic Zebrafish Test System

Audrey Bernut, Vincent Le Moigne, Tiffany Lesne, Georges Lutfalla,
Jean-Louis Herrmann, Laurent Kremer

► To cite this version:

Audrey Bernut, Vincent Le Moigne, Tiffany Lesne, Georges Lutfalla, Jean-Louis Herrmann, et al.. In Vivo Assessment of Drug Efficacy against Mycobacterium abscessus Using the Embryonic Zebrafish Test System. Antimicrobial Agents and Chemotherapy, 2014, 58 (7), pp.4054-4063. 10.1128/AAC.00142-14 . hal-02088311

HAL Id: hal-02088311

<https://hal.umontpellier.fr/hal-02088311>

Submitted on 11 Apr 2019

HAL is a multi-disciplinary open access archive for the deposit and dissemination of scientific research documents, whether they are published or not. The documents may come from teaching and research institutions in France or abroad, or from public or private research centers.

L'archive ouverte pluridisciplinaire **HAL**, est destinée au dépôt et à la diffusion de documents scientifiques de niveau recherche, publiés ou non, émanant des établissements d'enseignement et de recherche français ou étrangers, des laboratoires publics ou privés.

***In vivo* assessment of drug efficacy against *Mycobacterium abscessus* using the embryonic zebrafish test system**

**Audrey Bernut¹, Vincent Le Moigne³, Tiffany Lesne¹, Georges Lutfalla¹,
Jean-Louis Herrmann³ and Laurent Kremer^{1,2,#}**

¹Laboratoire de Dynamique des Interactions Membranaires Normales et Pathologiques, CNRS UMR5235, Université Montpellier 2, Montpellier, France ;

²Inserm, DIMNP, Place Eugène Bataillon, 34095 Montpellier Cedex 05, France.

³EA3647-EPIM, UFR des Sciences de La Santé; Université de Versailles St Quentin, 2 avenue de la Source de la Bièvre, 78180 Montigny le Bretonneux, France.

[#]To whom correspondence should be addressed:

Tel: (+33) 4 67 14 33 81, Fax: (+33) 4 67 14 42 86, E-mail: laurent.kremer@univ-montp2.fr

Keywords: *M. abscessus*, zebrafish, drug testing, optical imaging, infection

Running title: *In vivo* imaging for anti-*M. abscessus* drug testing

ABSTRACT

Mycobacterium abscessus is responsible of a wide spectrum of clinical syndromes and is one of the most intrinsically drug-resistant mycobacterial species. Recent evaluation of the *in vivo* therapeutic efficacy of the few potentially active antibiotics against *M. abscessus* was essentially performed using immune-compromised mice. Herein, we assessed the feasibility and sensitivity of fluorescence imaging for monitoring the *in vivo* activity of drugs against acute *M. abscessus* infection using zebrafish embryos. A protocol was developed where clarithromycin and imipenem were directly added to water containing fluorescent *M. abscessus*-infected embryos in a 96-well plate format. The status of the infection with increasing drug concentrations was visualized on a spatiotemporal level. Drug efficacy was assessed quantitatively by determining the index of protection, the bacterial burden by CFU plating and by monitoring the number of abscesses through fluorescence measurements. Both drugs were active in infected embryos and were capable of significantly increasing embryo survival in a dose-dependent manner. Protection from bacterial killing correlated with restricted mycobacterial growth in the drug-treated larvae and with reduced pathophysiological symptoms, such as the number of abscesses within the brain. In conclusion, we present here a new and efficient method for testing and compare the *in vivo* activity of two clinically-relevant drugs based on a fluorescent reporter strain in zebrafish embryos. This approach could be applied to a rapid determination of *in vivo* drug susceptibility profile of clinical isolates and to assess the preclinical efficacy of new compounds against *M. abscessus*.

INTRODUCTION

M. abscessus (*Mabs*) is an emerging pathogen and the etiological agent of a wide spectrum of infections in humans. It is responsible for severe chronic pulmonary and disseminated infections, mostly in immunosuppressed and in cystic fibrosis (CF) patients (1), and cutaneous diseases, often post-traumatic and post-surgical. This neglected pathogen causes a higher fatality rate compared to other RGMs and the infection of CF patients is becoming a major health-related issue in most CF centers worldwide (2). *Mabs* infections occur in early childhood (3), are severe and sometimes fatal, especially following transplantation (4-6), and have the potential to cause outbreaks of infection (6). *Mabs* is also the main RGM responsible for nosocomial and iatrogenic infections in humans (post-injection abscesses, cardiac surgery, and plastic surgery) (7-9). It has also been reported to cross the blood-brain barrier and to cause important central nervous system (CNS) lesions. Although a rapid grower, *Mabs* possesses several important pathogenic traits such as the ability to i) persist silently for years and even decades (10) in the human host, and to ii) induce lung disease associated with caseous lesions and granuloma formation in lung parenchyma (11, 12).

The major issue with *Mabs* relies on its intrinsic resistance to the majority of available antibiotics. The American Thoracic Society has recommended different groups of agents, namely macrolides (clarithromycin), aminoglycosides (amikacin), cephamycins (cefoxitin) and carbapenems (imipenem) for treatment of *Mabs* infections (13). Patients with severe infections are generally treated with long courses of combinatorial antibiotic therapy, often accompanied by surgical resection. As antibiotic susceptibility testing is not fully standardized, the clinical response to drugs does not correlate well with *in vitro* susceptibility test results and failure occurs frequently despite administration of two or three antibiotics for several months (14).

This further emphasizes the need of suitable animal models (15, 16). In addition, different clinical isolates of this emerging pathogen are not uniformly susceptible to the currently used antibiotics (17). As a consequence, an optimal regimen to cure the *Mabs* infections has not been yet established.

Thanks to the recent availability of efficient genetic tools (18), *Mabs* has been proposed as an attractive experimental model to study non-tuberculous mycobacteria associated diseases (1). Our poor understanding of the pathogenesis of *Mabs*, essentially hampered by the restricted panel of cellular/animal models available, prompted us to develop the zebrafish model of infection to describe the chronology of *Mabs* infection (19). In particular, the *Mabs*/zebrafish couple already provided important insights regarding the pathogenesis of *Mabs* such as the unexpected tropism for the CNS, a finding relevant in the light of recent clinical studies reporting the presence of *Mabs* in the CNS of infected human patients (20, 21). Since infection foci/abscesses within the CNS, particularly the brain, appear very rapidly and are very easy to detect and visualize, we reasoned that this alternative model could represent a valuable and cheap system to evaluate and compare the *in vitro* and *in vivo* activity of drugs against *Mabs*. Such a simple and innovative system would be particularly suited for screening active molecules and/or antibacterial activity assessment, representing a critical step in the context of drug discovery, urgent in the case of *Mabs*.

Here, we report on the development of experimental conditions for *in vivo* imaging of *Mabs* and demonstrate that it is compatible with *in vivo* observations, at a spatiotemporal level, of the effects of drug treatment on the infection process. This represents a unique biological model that allows non-invasive observations to evaluate, in real time, the efficacy of antibiotics in living infected vertebrates, a system that could be applied to high-throughput *in vivo* testing of drug efficacy against the most drug-resistant mycobacterial species.

MATERIALS AND METHODS

***M. abscessus* strains and growth conditions**

The rough variant of *M. abscessus sensu stricto* strain CIP104536^T (ATCC19977T) was grown at 30°C in Middlebrook 7H9 broth supplemented with 10% Oleic acid/Albumin/Dextrose/Catalase (OADC) enrichment and 0.05% Tween 80 (7H9^T) or on Middlebrook 7H10 agar containing 10% OADC. Recombinant *Mabs* carrying pTEC27 (Addgene, plasmid 30182) that allows to express tdTomato under the control of a strong mycobacterial promoter were grown in the presence of hygromycin 500 mg/L (19).

Mice experiments and CFU counting

6-8 weeks old BALB/c mice were divided in groups of 5-7 mice and used for either intravenous (*i.v.*) or aerosol challenges. Inocula were prepared from rapidly thawed frozen aliquots, and bacterial clumps were eliminated by iterative passages through a 29.5-gauge insulin needle (Becton Dickinson). Bacterial suspensions were then diluted in phosphate buffer saline (PBS). For *i.v.* inoculations, 10⁶ CFU (in 200 µl) were injected into the lateral tail/caudal vein, as previously described (22, 23). Pulmonary infections were achieved with aerosolized *Mabs* using an aerosol generator, equipped with a Micro Mist[®] small volume nebulizer (Hudson RCI-Teleflex medical) containing 6 ml of bacterial solution at 4 × 10⁷ CFU/ml. Pre-sleeping mice (isoflurane[®] Abbott) were anesthetized with 200 µl of Hypnomidate (Etomidate[®], Janssen-Cilag) and placed into an opened 50 ml syringe fixed on the top of a closed compartment containing the nebulizer. In this device, nebulization lasted for 15 min to vaporize the entire bacterial suspension. Lungs, liver and spleen were collected in PBS, crushed and 10-folds serial dilutions were plated on Middlebrook 7H11 plates for CFU counting, as previously described (22, 23).

Plates were then incubated at 37°C for up to 7 days. The results were expressed as the mean Log₁₀ CFU per organ.

Minimal inhibitory concentrations

Antibiotics powder tested in drug susceptibility assays were pharmaceutical standards for imipenem/cilastatin (Mylan) or clarithromycin (Sigma-Aldrich). Stock solutions were dissolved in water (imipenem) or in DMSO (clarithromycin). Drug susceptibility testing was also determined using the microdilution method, in cation-adjusted Mueller-Hinton broth, according to the Clinical and Laboratory Standards Institute (CLSI) guidelines (24). In addition, the susceptibility profile was also determined on LB agar supplemented with increasing concentrations of the compounds. Serial 10-fold dilutions of each actively growing culture were plated and incubated at 37°C for 3-4 days and the MIC was defined as the minimum concentration required to inhibiting 99% of the growth.

Zebrafish care

All zebrafish experiments were done at the University Montpellier 2, according to European Union guidelines for handling of laboratory animals (http://ec.europa.eu/environment/chemicals/lab_animals/home_en.htm) and approved by the Direction Sanitaire et Vétérinaire de l'Hérault and Comité d'Ethique pour l'Expérimentation Animale de la région Languedoc Roussillon (CEEALR) under the reference CEEALR-13007. Experiments were performed using the *golden* ZF mutant (25). Eggs were obtained by natural spawning and incubated at 28.5°C in water with 60 mg/L Ocean salts. Ages of the embryos are expressed as hours post fertilization (hpf).

Microinjection of *M. abscessus* into embryos

Mid-log phase cultures of *Mabs* expressing tdTomato were centrifuged, washed and resuspended in PBS supplemented with 0.05% Tween-80 (PBS^T). Bacterial suspensions were then homogenized through a 26-gauge needle and sonicated three times for 10s and the remaining clumps were allowed to settle down to for 5-10 min. Bacteria were concentrated to an OD₆₀₀ of 1 in PBS^T and *i.v.* injected (≈2nL containing 300 CFU) into the caudal vein in 30hpf embryos previously dechorionated and anesthetized. To follow infection kinetics and embryo survival, infected larvae were transferred into 96 well plates (2 embryos/plate) and incubated at 28.5°C. The inoculum size was checked by injection of 2nL in sterile PBS^T and plated on Middlebrook 7H10 agar containing 10% OADC supplemented with hygromycin 500 mg/L.

Drug efficacy assessment in *Mabs*-infected ZF

Clarithromycin and imipenem/cilastatin were added at one day post-infection (dpi), directly into the water containing the embryos. Three doses were tested, corresponding to 1.7X, 17X and 170X the MIC of clarithromycin and 0.5X, 5X or 28X the MIC of imipenem, based on the values determined using the microdilution method (Table S1). *In vivo* drug efficacy was determined for each concentration by following i) the bacterial burdens, ii) the kinetic of embryo survival, iii) the evolution of the infection foci/abscesses within the CNS and iv) the effect on bacterial cord formation/reduction. Survival curves were determined by recording dead embryos (no heartbeat) every day for up to 13 days. Regarding the kinetic of mycobacterial loads, groups of three infected embryos were collected, lysed individually in 2% Triton X100- PBS^T with a 26-gauge needle (15 up-and-down sequences) and resuspended in PBS^T. Several 10-fold dilutions of homogenates were plated on Middlebrook 7H10 agar supplemented with 10% OADC, the appropriate antibiotics and added of mix of “BBL™ MGIT™

PANTA™ (Becton-Dickinson) using as recommended by the supplier. CFU were enumerated after 4 days of incubation at 30°C. This procedure was repeated at 0, 3, 5 dpi.

Microscopy

Widefield bright-field and fluorescence live microscopy of infected embryos were performed using an Olympus MVX10 epifluorescent microscope equipped with a X-Cite® 120Q (Lumen Dynamics) 120W mercury light source. Images are acquired with a digital color camera (Olympus XC50) and processed using CellSens software (Olympus). Fluorescence filter cube TRITC-MVX10 is used for detection of red light. For live imaging, anesthetized infected embryos were positioned in dishes and immobilized with 1% low-melting point agarose solution covering the entire larvae then immobilized embryos are immersed with fish water containing tricaine for direct visualization.

Image Processing and Analysis

Final images analysis and visualization are performed using GIMP 2.6 freeware to merge fluorescent and DIC images and to adjust levels and brightness and to remove out-of-focus background fluorescence.

Statistical Analyses

Statistical analyses of comparisons between Kaplan-Meier survival curves were performed using the log rank test with Prism 4.0 (Graphpad, Inc). CFU counts and quantifications experiments were analyzed using one-way ANOVA and Fisher's exact test, respectively. Statistical significance was assumed at p values <0.05 .

RESULTS

***M. abscessus* fails to establish a persistent infection in BALB/c mice**

Experiments were first aimed to determine the colonization rate of *Mabs* in a murine pulmonary infection model (Figure 1A). Aerosol infections of BALB/c mice was characterized by an initial and rapid increase of the bacterial burden from 1-3 days post-infection (dpi) in the lungs, followed by a phase of infection control that leads to a reduction (starting after 3dpi) and almost complete clearance of the bacilli at 27dpi. Very few bacteria were detected within the spleen or the liver of infected mice. The colonization profile after an *i.v.* challenge showed that bacilli were primarily found in the liver at 1dpi and to a lesser extent in the spleen and the lungs (Figure 1B). All heavily infected organs rapidly underwent a progressive reduction in the CFU levels with a 3-Log₁₀ CFU decrease in the liver and the lungs at 30dpi, highlighting a transient colonization process. These results indicate that the course of infection in immune-competent mice consists mostly as a progressive eradication of the pathogen. This model would, therefore, require to testing a very large number of animals to insure that the observed CFU decrease results to the antibiotic regimen rather than to the natural course of infection. Consequently, wild-type BALB/c mice are not well adapted to investigate the *in vivo* efficacy of therapeutic treatments. Therefore, the use of alternative animal models susceptible to *Mabs* infection, permissive to bacterial replication and leading to the development of infection foci/abscesses and death would be particularly advantageous. We hypothesized that ZF larvae may represent a valuable system for *in vivo* assessments of drugs against *Mabs*.

Zebrafish larvae for *in vivo* assessment of drug activity in *M. abscessus*

To assess *in vivo* antimycobacterial drug activity against *Mabs* in ZF larvae, an experimental protocol has been established (Figure 2). tdTomato-expressing *Mabs*, exhibiting red

fluorescence, were *i.v.* injected in the caudal vein of embryos at 30 hours post-fertilization (hpf) and transferred into 96-well plates. Antibiotic were then directly added at 1dpi to the water containing the infected embryos and the drug-supplemented water was then changed on a daily basis for 5 days. Daily monitoring of mortality as well as determination of the bacterial burden at various time points were used as phenotypic read-outs. Thanks to the optical transparency of the embryos, the effect of the antibiotic treatment on evolution of the clinical signs of infection was also recorded by fluorescence microscopy. Since most infected *Mabs* infected-embryos developed infection abscesses within the CNS, especially the brain (Figure 2), the chemotherapeutic activity of the antibiotics was particularly easy to observe, on an individual basis, during the entire period of drug treatment. Drug-mediated toxicity was also investigated by determining the survival curves of non-infected embryos treated with increasing drug doses. We have previously shown that the rough *Mabs* exhibits a marked neurotropism with massive abscesses within the CNS (19), thus prompting us to assess the activity of drugs in *Mabs*-infected embryos with a special emphasis on infection within the CNS.

Minimal inhibitory concentrations of antimycobacterial drugs against *M. abscessus*

We first determined the *in vitro* activity of various drugs, including antitubercular agents, against *Mabs* using the microdilution in cation-adjusted Mueller-Hinton broth, according to the Clinical and Laboratory Standards Institute guidelines (24). Table S1 shows that the activity varies considerably, in agreement with other studies. The first-line antitubercular drug isoniazid and second-line drug thiacetazone appeared inactive against *Mabs*. Among the few clinically used drugs for the treatment of *Mabs* infection, cefoxitin, amikacin, imipenem and erythromycin exhibit moderate activity *in vitro* on agar plates with MICs ranging from 60-125 μ M, whereas clarithromycin demonstrated the highest activity with an MIC value of 4 μ M.

Because clarithromycin and imipenem exhibit different physicochemical properties (high molecular weight and hydrophobicity for clarithromycin versus low molecular weight and hydrophilicity for imipenem), they were further investigated for their *in vivo* therapeutic efficacy in *Mabs*-infected ZF.

***In vivo* susceptibility of *M. abscessus* to clarithromycin**

Due to insufficient information concerning the mechanisms of drug uptake by ZF embryos/larvae, a wide range of concentrations, spanning from 6.6 μ M-668 μ M of clarithromycin (corresponding to 1.7X to 170X the *in vitro* MIC value obtained using the microdilution method) was tested. Supplementation of the embryo-containing water with low or intermediate doses (1.7X and 17X the MIC, respectively) displayed no toxicity as measured by larval survival, while used at the highest dose tested (170X MIC), a 10% reduction in larval survival was observed at 9dpi, with respect to the control group in which water was supplemented with 1% DMSO (26) (Figure 3A). Embryos that develop in the presence of high doses of clarithromycin had a curved body trunk with uninflated swim bladder as compared to the DMSO control embryos (Figure 3A, inset). These phenotypic alterations were hardly observed when exposed to intermediate or low doses of clarithromycin (data not shown).

Nevertheless, since these developmental abnormalities essentially occurred at the highest doses, we next assessed the *in vivo* efficacy of clarithromycin in *Mabs*-infected embryos. No significant increased survival was found when infected-embryos were exposed to low and intermediate drug concentrations (Figure 3B). In contrast, high doses extended the life span of infected embryos and fully protected the infected embryos up to 9dpi, when the first embryo started to dye, which coincidentally, corresponded to the toxicity-induced-killing effect (Figure 3A). This shows that clarithromycin, using the highest regimen, is efficient in the ZF test system.

Effects of clarithromycin on ZF survival, bacterial burden and abscesses

Increased survival was associated with lower bacterial burdens after 3dpi in the presence of the highest dose (170X MIC), as determined quantitatively by CFU plating (Figure 3C), whereas treatment with the low or intermediate doses failed to restrict mycobacterial growth. *In vivo* drug efficacy was next monitored by time-lapse fluorescence microscopy (Figure 3D). Injection of *Mabs* led to the appearance of rapidly growing infection foci and abscesses in the larval brain at 3dpi, as reported previously (19). Imaging the same infected embryos at 3 and 5dpi revealed that abscesses within the brain were already reduced at 3dpi when treated with high drug concentrations and this effect in reducing the clinical signs of the infection was even more accentuated at 5dpi. There was no visible reduction of the infection at 5dpi in ZF treated with low or intermediate drug concentrations, consistent with the survival curves and kinetic of bacterial growth. A quantitative analysis revealed that high doses of clarithromycin reduced by 50% the number of embryos with abscesses (Figure 3E), and this drug effect was apparent in both the brain and the spinal cord (Figure 3F), albeit the impact of lower drug concentrations was not significant. This indicates that clarithromycin exerts a beneficial effect by inhibiting mycobacterial growth, preventing the development of abscesses within the CNS and protecting the embryos from bacterial killing.

Effects of imipenem on ZF survival and reduction of the pathological signs

To further confirm and extend the impact and usefulness of this biological system with respect to *in vivo* drug testing, embryos were exposed to water-soluble imipenem, a clinically relevant drug against *Mabs* known to act on L,D-transpeptidases (17, 27). A wide range of concentrations was tested, corresponding to 0.5X to 28X MIC of imipenem, and neither signs of toxicity-induced-killing nor developmental abnormalities were detected even at the highest

dose (data not shown). When assessing the effect of imipenem on infected ZF, no increased survival was found with low drug concentrations. However, treatment with intermediate doses led to a significant increase in survival and 100% of protection was observed in the presence of this highest drug concentration (Figure 4A). These survival rates correlated with the CFU loads as intermediate and high doses of imipenem started to restrict bacterial growth at 3dpi (after two days of drug treatment) (Figure 4B). With the highest dose, there was a 3 Log₁₀ decline in the CFU at 5dpi (four days of treatment) compared with the untreated control group. Time-lapse fluorescence microscopy further confirmed the *in vivo* efficacy of imipenem, illustrating the inhibition of bacterial growth and disappearance of abscesses in the larval brain at 3 and 5dpi, respectively (Figure 4C). There was no visible reduction of the infection at 5dpi when treated with low imipenem doses, consistent with the survival curves and kinetic of bacterial growth. High doses significantly reduced the proportion of embryos with abscesses (Figure 4D), a phenotypic effect that was particularly apparent in the brain on infected embryos (Figure 4E), indicating that imipenem reduces the pathology signs of the infection.

These results also prompted us to examine whether imipenem can counteract/alter the progression of an already established infection, especially when given at 3dpi when brain abscesses are already apparent (Figure S1A). Death curves indicate that treatment with high doses of imipenem effectively extended the life span of embryos with pre-existing abscesses (Figure S1B). A large proportion (more than 60%) of the treated embryos survived to the infection compared to 10% for the non-treated individuals ($P=0.008$). The remaining 40% embryos that died despite the treatment showed increased bacterial loads in the CNS (data not shown). The increased index of protection rate was associated to a significant decrease in the number of embryos with abscesses (Figure S1C), particularly within the brain (Figure S1D). This

“curative” protocol shows that imipenem was able to cure embryos with pre-existing abscesses and to protect severely infected ZF.

***In vivo* inhibition activity of imipenem on mycobacterial cording**

Rough *Mabs* displays a dry texture with organized serpentine cords on agar plates (19, 28, 29) and large bacterial clumps consisting mainly of cords in liquid cultures (19). Our recent studies also unraveled the presence of serpentine cords within the brain or spinal cord of embryos infected with the rough morphotype and emphasized the role of cording in immune evasion by preventing phagocytosis of *Mabs* by macrophages and neutrophils (19). Since cords are easy to visualize and to numerate by fluorescence microscopy (Figure 5A), and because they promote extracellular replication, abscess formation and tissue damage, we investigated whether exposure of infected embryos to imipenem may also affect the development of mycobacterial cords. Figure 5B shows the presence of multiple cords within the brain at 5dpi (left panel) and the impact of imipenem treatment on the number of cords (right panel).

Quantitative analysis of the percentage of embryos with cords at 4dpi is shown in Figure 5C. The presence of low doses of imipenem has little impact on mycobacterial cords, although a reduction of the number of embryos with cords was detected at 4dpi. However, this effect was more pronounced with higher drug concentrations with only 20% of cord-laden embryos at 4dpi (compared to 60% for untreated embryos at 4dpi). This dose-dependent effect occurred essentially within the CNS whilst reduction of cord formation within the vasculature was not significant (Figure 5D).

DISCUSSION

At a basic research level, the appropriate use of animal models can help to improve our understanding of host-pathogen interactions. At a more applied level, preclinical evaluation of new drug compounds requires *in vivo* testing prior these can advance along the development pipeline. However, *in vivo* animal studies, when possible, are usually costly and time-consuming and present a major bottleneck in drug developments. Implementation of novel approaches, expected to accelerate the *in vivo* efficacy assessment of drugs, is particularly justified in two cases. First, such systems are useful for bacterial infections requiring extended periods of drug treatment such as mice infected with *M. tuberculosis*, for which rapid *in vivo* assessment of drug efficacy directly in infected mice using fluorescence imaging (30) or using improved firefly luciferase (31) were elegantly demonstrated. We similarly show in this study how the use of fluorescence imaging can be useful in evaluating antimicrobial activity against *Mabs*. Second, alternative biological systems are particularly relevant for infections lacking of a permissive animal model. In this context, we recently demonstrated the high susceptibility of ZF embryos to *Mabs* and how the number of CNS abscesses may represent a marker for establishing *in vivo* antibiotic activity against *Mabs*.

Due to its intrinsic and acquired resistance to commonly used antibiotics, treatment becomes more complicated, thereby leading to high failure rates, stressing the need for new drug discovery. One of the key steps of drug discovery process is to identify and evaluate the *in vitro* and *in vivo* potential of new hits against *Mabs*, which pre-requires adequate animal models. Assessing the murine model which, following *i.v.* or aerosol infection, led only to transient colonization. Therefore, the natural course of infection in immune-competent BALB/c mice impedes its use as a valuable animal model for drug susceptibility testing. Comparatively, SCID mouse model has been shown to produce a chronic infection of *Mabs*, but this model has

not been used for drug testing (29, 32). However, granulocyte-macrophage colony-stimulating (GM-CSF) knockout mice have recently been used to develop a new animal model of persistent pulmonary *Mabs* infection that can be used for preclinical efficacy testing of anti-microbial drugs (15). In particular, azithromycin treatment of *Mabs*-infected GM-CSF KO mice resulted in a lower bacterial burden in the lungs and spleen, weight gain and significant improvement in lung pathology (15). Another report proposed Nude mice as an adequate model for *in vivo* chemotherapy studies (16). However, both models raised the question of the adaptive response in addition to the antibiotic activity in eradicating the bacilli. It was previously shown that, albeit being a rapid-growing mycobacterium, *Mabs* infection was only controlled in mice with a functional adaptive immune response (22), as compared to *M. chelonae*, which was cleared even in T cell-deficient mice. In addition, and despite the fact that both immune-compromised mice present a significant advance as compared to wild-type mice in preclinical assessments, these models remain costly and time-consuming and remain most likely not suitable for a general use in drug screening campaigns.

New non-mammalian models of infection have been developed, including *Drosophila melanogaster* (33, 34), *Caenorhabditis elegans* (35) or *Danio rerio* (36, 37) which offer several advantages in terms of speed, cost, technical convenience and ethical acceptability over the mouse model. However, very few of these alternative models, except for the recent *Drosophila* model (34), have been reported for antibiotic assessments against *Mabs*. In this study, we propose the ZF model, to visualize by non-invasive imaging the progressive infection of *Mabs* in live animals, and to quantifying the effect of drug treatment. We successfully investigated the suitability and sensitivity of two clinically relevant drugs, clarithromycin and imipenem, to visualize in a dose- and time-dependent manner the dynamics of cord and abscess formation/resorption. One major advantage of this model compared to mice is the ease and

rapidity of experimentation within a restricted time scale and low cost. That both drugs had a positive impact in terms of embryo survival was correlated to a significant reduction in the number of CFU and abscesses, demonstrating a proof of concept that ZF embryos are suitable for drug efficacy testing. Since *in vitro* studies demonstrated decreased MICs in the presence of imipenem for clarithromycin, minocycline, levofloxacin and moxifloxacin (38), future work should also address the *in vivo* efficacy of these drug combinations using the *Mabs*/ZF couple.

It is, however, noteworthy that despite of their unique features for the *in vivo* drug testing, ZF embryos also present several disadvantages over mammalian models. In particular, there are some important anatomical differences between ZF embryos and mammals such as gills instead of lungs, hematopoiesis occurring in the anterior kidney instead of the bone marrow, lack on discernable lymph nodes as well as a very different reproductive system. In addition, the natural lack of an adaptive immunity early in the development is very likely to affect the outcome of the infection, thus making it difficult to directly correlating data obtained in ZF and in humans. In addition, as shown in this study, embryos allow to describing effects of antibiotics during acute *Mabs* infections but not during the chronic stages of the disease, which can be better modelled for instance using immuno-compromized mice (15). In a similar vein, since pharmacokinetics in are not known in ZF, it remains difficult at this stage to directly transpose the MIC data obtained in ZF to humans. As a consequence, this biological system should essentially be regarded as an early model for pre-clinical drug testing and/or to select for new active compounds which should then be evaluated in other models before clinical trials.

Nevertheless, the perspectives of application of these findings are multiple. First, this method could be implemented to address the *in vivo* drug susceptibility profiles of clinical isolates that include strains from CF and non-CF patients, as *Mabs* clinical strains are not uniformly susceptible to the currently used antibiotics. Due to these strain-to-strain variations

(17, 39), no optimal regimen has been established to cure *Mabs* infections and determining the susceptibility/resistance profile of clinical strains may greatly help the clinician to select optimal drug treatments. It is worth mentioning that for this particular application, no absolute requirement for the tested strains to carry pTEC27 is needed, as visualization of fluorescent bacteria is not necessary if assessing ZF survival only. Second, since the ZF is particularly amenable to mimic a CF-like micro-environment, by silencing the *cftr* expression level (40), this system would also allow to comparing the therapeutic efficacy of clarithromycin and imipenem (and perhaps other antibiotics) in a *cftr*-deficient environment as it remains to be established whether a defect in CFTR affects susceptibility to drugs. Third, this method could be further exploited to compare the intrinsic activity of antibiotics *in vivo* in embryos infected with the three species of the *M. abscessus* complex - *M. abscessus sensu stricto*, *M. massiliense*, and *M. bolletii* - which are known to respond differently to antibiotics *in vitro* (41, 42).

Finally, the ZF embryo is particularly suited for high throughput screening as shown recently for *M. marinum* (36, 43, 44). Work is currently in progress in our laboratory to develop an *in vivo* platform for high-throughput screening of molecules against *Mabs* in order to speed up the process of identifying promising drug candidates, particularly warranted due to the extreme resistance of *Mabs* to most current antibiotics.

ACKNOWLEDGMENTS

We thank L. Ramakrishnan for the generous gift of pTEC27 and for helpful discussions and the Montpellier RIO Imaging and the SCME facilities at UM2.

This study was supported by the french National Research Agency (<http://www.agence-nationale-recherche.fr/>) (ZebraFlam ANR-10-MIDI-009 and DIMYVIR ANR-13-BSV3-0007-01), the European Community's Seventh Framework Programme (FP7-PEOPLE-2011-ITN) under grant agreement no. PITN-GA-2011-289209 for the Marie-Curie Initial Training Network FishForPharma. We wish also to thank Vaincre La Mucoviscidose (<http://www.vaincrelamuco.org/>) for funding A Bernut (RF2011 06000446) and V Le Moigne (RF20120600689) and the InfectioPôle Sud for funding part of the fish facility.

REFERENCES

1. **Medjahed, H., J. L. Gaillard, and J. M. Reytrat.** 2010. Mycobacterium abscessus: a new player in the mycobacterial field. Trends Microbiol **18**:117-23.
2. **Petrini, B.** 2006. Mycobacterium abscessus: an emerging rapid-growing potential pathogen. Apmis **114**:319-28.
3. **Roux, A. L., E. Catherinot, F. Ripoll, N. Soismier, E. Macheras, S. Ravilly, G. Bellis, M. A. Vibet, E. Le Roux, L. Lemonnier, C. Gutierrez, V. Vincent, B. Fauroux, M. Rottman, D. Guillemot, and J. L. Gaillard.** 2009. Multicenter study of prevalence of nontuberculous mycobacteria in patients with cystic fibrosis in france. J Clin Microbiol **47**:4124-8.
4. **Sanguinetti, M., F. Ardito, E. Fiscarelli, M. La Sorda, P. D'Argenio, G. Ricciotti, and G. Fadda.** 2001. Fatal pulmonary infection due to multidrug-resistant Mycobacterium abscessus in a patient with cystic fibrosis. J Clin Microbiol **39**:816-9.
5. **Gilljam, M., H. Schersten, M. Silverborn, B. Jonsson, and A. Ericsson Hollsing.** 2010. Lung transplantation in patients with cystic fibrosis and Mycobacterium abscessus infection. J Cyst Fibros **9**:272-6.
6. **Aitken, M. L., A. Limaye, P. Pottinger, E. Whimbey, C. H. Goss, M. R. Tonelli, G. A. Cangelosi, M. A. Dirac, K. N. Olivier, B. A. Brown-Elliott, S. McNulty, and R. J. Wallace, Jr.** 2012. Respiratory outbreak of Mycobacterium abscessus subspecies massiliense in a lung transplant and cystic fibrosis center. Am J Respir Crit Care Med **185**:231-2.
7. **Wallace, R. J., Jr., B. A. Brown, and D. E. Griffith.** 1998. Nosocomial outbreaks/pseudo-outbreaks caused by nontuberculous mycobacteria. Annu Rev Microbiol **52**:453-90.
8. **Viana-Niero, C., K. V. Lima, M. L. Lopes, M. C. Rabello, L. R. Marsola, V. C. Brilhante, A. M. Durham, and S. C. Leao.** 2008. Molecular characterization of Mycobacterium massiliense and Mycobacterium bolletii in isolates collected from outbreaks of infections after laparoscopic surgeries and cosmetic procedures. J Clin Microbiol **46**:850-5.

9. **Zelazny, A. M., J. M. Root, Y. R. Shea, R. E. Colombo, I. C. Shamputa, F. Stock, S. Conlan, S. McNulty, B. A. Brown-Elliott, R. J. Wallace, Jr., K. N. Olivier, S. M. Holland, and E. P. Sampaio.** 2009. Cohort study of molecular identification and typing of *Mycobacterium abscessus*, *Mycobacterium massiliense*, and *Mycobacterium bolletii*. *J Clin Microbiol* **47**:1985-95.
10. **Cullen, A. R., C. L. Cannon, E. J. Mark, and A. A. Colin.** 2000. *Mycobacterium abscessus* infection in cystic fibrosis. Colonization or infection? *Am J Respir Crit Care Med* **161**:641-5.
11. **Tomashefski, J. F., Jr., R. C. Stern, C. A. Demko, and C. F. Doershuk.** 1996. Nontuberculous mycobacteria in cystic fibrosis. An autopsy study. *Am J Respir Crit Care Med* **154**:523-8.
12. **Rodriguez, G., M. Ortegon, D. Camargo, and L. C. Orozco.** 1997. Iatrogenic *Mycobacterium abscessus* infection: histopathology of 71 patients. *Br J Dermatol* **137**:214-8.
13. **Griffith, D. E., T. Aksamit, B. A. Brown-Elliott, A. Catanzaro, C. Daley, F. Gordin, S. M. Holland, R. Horsburgh, G. Huitt, M. F. Iademarco, M. Iseman, K. Olivier, S. Ruoss, C. F. von Reyn, R. J. Wallace, Jr., and K. Winthrop.** 2007. An official ATS/IDSA statement: diagnosis, treatment, and prevention of nontuberculous mycobacterial diseases. *Am J Respir Crit Care Med* **175**:367-416.
14. **Jeon, K., O. J. Kwon, N. Y. Lee, B. J. Kim, Y. H. Kook, S. H. Lee, Y. K. Park, C. K. Kim, and W. J. Koh.** 2009. Antibiotic treatment of *Mycobacterium abscessus* lung disease: a retrospective analysis of 65 patients. *Am J Respir Crit Care Med* **180**:896-902.
15. **De Groote, M. A., L. Johnson, B. Podell, E. Brooks, R. Basaraba, and M. Gonzalez-Juarrero.** 2013. GM-CSF knockout mice for preclinical testing of agents with antimicrobial activity against *Mycobacterium abscessus*. *J Antimicrob Chemother* **In Press**.
16. **Lerat, I., E. Cambau, R. Roth Dit Bettoni, J. L. Gaillard, V. Jarlier, C. Truffot, and N. Veziris.** 2013. In vivo evaluation of antibiotic activity against *Mycobacterium abscessus*. *J Infect Dis* **In Press**.
17. **Lavollay, M., V. Dubee, B. Heym, J. L. Herrmann, J. L. Gaillard, L. Gutmann, M. Arthur, and J. L. Mainardi.** 2013. In vitro activity of cefoxitin and imipenem against *Mycobacterium abscessus* complex. *Clin Microbiol Infect* **In Press**.

- 483 18. **Cortes, M., A. K. Singh, J. M. Reyrat, J. L. Gaillard, X. Nassif, and J. L. Herrmann.** 2011.
484 Conditional gene expression in *Mycobacterium abscessus*. *PLoS One* **6**:e29306.
- 485 19. **Bernut, A., J. L. Herrmann, K. Kissa, J. F. Dubremetz, J. L. Gaillard, G. Lutfalla, and L. Kremer.**
486 The zebrafish model reveals specific pathophysiological traits and neurotropism of
487 *Mycobacterium abscessus*. **Under revision.**
- 488 20. **Talati, N. J., N. Rouphael, K. Kuppalli, and C. Franco-Paredes.** 2008. Spectrum of CNS disease
489 caused by rapidly growing mycobacteria. *Lancet Infect Dis* **8**:390-8.
- 490 21. **Lee, M. R., A. Cheng, Y. C. Lee, C. Y. Yang, C. C. Lai, Y. T. Huang, C. C. Ho, H. C. Wang, C. J. Yu,**
491 **and P. R. Hsueh.** 2011. CNS infections caused by *Mycobacterium abscessus* complex: clinical
492 features and antimicrobial susceptibilities of isolates. *J Antimicrob Chemother* **67**:222-5.
- 493 22. **Rottman, M., E. Catherinot, P. Hochedez, J. F. Emile, J. L. Casanova, J. L. Gaillard, and C.**
494 **Soudais.** 2007. Importance of T cells, gamma interferon, and tumor necrosis factor in immune
495 control of the rapid grower *Mycobacterium abscessus* in C57BL/6 mice. *Infect Immun* **75**:5898-
496 907.
- 497 23. **Catherinot, E., J. Clarissou, G. Etienne, F. Ripoll, J. F. Emile, M. Daffe, C. Perronne, C. Soudais, J.**
498 **L. Gaillard, and M. Rottman.** 2007. Hypervirulence of a rough variant of the *Mycobacterium*
499 *abscessus* type strain. *Infect Immun* **75**:1055-8.
- 500 24. **Woods, G. L., B. A. Brown-Elliott, P. S. Conville, E. P. Desmond, G. S. Hall, G. Lin, G. E. Pfyffer, J.**
501 **C. Ridderhof, S. H. Siddiqi, R. J. Wallace, N. G. Warren, and F. G. Witebsky.** 2011. Susceptibility
502 testing of mycobacteria, nocardiae, and other aerobic actinomycetes; approved standard,
503 Second Edition. M24-A2. Clinical and Laboratory Standards Institute, Wayne, PA.
- 504 25. **Lamason, R. L., M. A. Mohideen, J. R. Mest, A. C. Wong, H. L. Norton, M. C. Aros, M. J. Juryneec,**
505 **X. Mao, V. R. Humphreville, J. E. Humbert, S. Sinha, J. L. Moore, P. Jagadeeswaran, W. Zhao, G.**
506 **Ning, I. Makalowska, P. M. McKeigue, D. O'Donnell, R. Kittles, E. J. Parra, N. J. Mangini, D. J.**
507 **Grunwald, M. D. Shriver, V. A. Canfield, and K. C. Cheng.** 2005. SLC24A5, a putative cation
508 exchanger, affects pigmentation in zebrafish and humans. *Science* **310**:1782-6.

- 509 26. **Adams, K. N., K. Takaki, L. E. Connolly, H. Wiedenhoft, K. Winglee, O. Humbert, P. H. Edelstein,**
510 **C. L. Cosma, and L. Ramakrishnan.** 2011. Drug tolerance in replicating mycobacteria mediated
511 by a macrophage-induced efflux mechanism. *Cell* **145**:39-53.
- 512 27. **Lavollay, M., M. Fourgeaud, J. L. Herrmann, L. Dubost, A. Marie, L. Gutmann, M. Arthur, and J.**
513 **L. Mainardi.** 2011. The peptidoglycan of *Mycobacterium abscessus* is predominantly cross-
514 linked by L,D-transpeptidases. *J Bacteriol* **193**:778-82.
- 515 28. **Medjahed, H., and J. M. Reytrat.** 2009. Construction of *Mycobacterium abscessus* defined
516 glycopeptidolipid mutants: comparison of genetic tools. *Appl Environ Microbiol* **75**:1331-8.
- 517 29. **Howard, S. T., E. Rhoades, J. Recht, X. Pang, A. Alsup, R. Kolter, C. R. Lyons, and T. F. Byrd.**
518 2006. Spontaneous reversion of *Mycobacterium abscessus* from a smooth to a rough
519 morphotype is associated with reduced expression of glycopeptidolipid and reacquisition of an
520 invasive phenotype. *Microbiology* **152**:1581-90.
- 521 30. **Zelmer, A., P. Carroll, N. Andreu, K. Hagens, J. Mahlo, N. Redinger, B. D. Robertson, S. Wiles, T.**
522 **H. Ward, T. Parish, J. Ripoll, G. J. Bancroft, and U. E. Schaible.** 2012. A new in vivo model to test
523 anti-tuberculosis drugs using fluorescence imaging. *J Antimicrob Chemother* **67**:1948-60.
- 524 31. **Andreu, N., A. Zelmer, S. L. Sampson, M. Ikeh, G. J. Bancroft, U. E. Schaible, S. Wiles, and B. D.**
525 **Robertson.** 2013. Rapid in vivo assessment of drug efficacy against *Mycobacterium tuberculosis*
526 using an improved firefly luciferase. *J Antimicrob Chemother*.
- 527 32. **Byrd, T. F., and C. R. Lyons.** 1999. Preliminary characterization of a *Mycobacterium abscessus*
528 mutant in human and murine models of infection. *Infect Immun* **67**:4700-7.
- 529 33. **Oh, C. T., C. Moon, M. S. Jeong, S. H. Kwon, and J. Jang.** 2013. *Drosophila melanogaster* model
530 for *Mycobacterium abscessus* infection. *Microbes Infect*.
- 531 34. **Oh, C. T., C. Moon, O. K. Park, S. H. Kwon, and J. Jang.** 2014. Novel drug combination for
532 *Mycobacterium abscessus* disease therapy identified in a *Drosophila* infection model. *J*
533 *Antimicrob Chemother*.

- 534 35. **Squiban, B., and C. L. Kurz.** 2011. *C. elegans*: an all in one model for antimicrobial drug
535 discovery. *Curr Drug Targets* **12**:967-77.
- 536 36. **Takaki, K., C. L. Cosma, M. A. Troll, and L. Ramakrishnan.** 2012. An in vivo platform for rapid
537 high-throughput antitubercular drug discovery. *Cell Rep* **2**:175-84.
- 538 37. **Takaki, K., J. M. Davis, K. Winglee, and L. Ramakrishnan.** 2013. Evaluation of the pathogenesis
539 and treatment of *Mycobacterium marinum* infection in zebrafish. *Nat Protoc* **8**:1114-24.
- 540 38. **Miyasaka, T., H. Kunishima, M. Komatsu, K. Tamai, K. Mitsutake, K. Kanemitsu, Y. Ohisa, H.**
541 **Yanagisawa, and M. Kaku.** 2007. In vitro efficacy of imipenem in combination with six
542 antimicrobial agents against *Mycobacterium abscessus*. *Int J Antimicrob Agents* **30**:255-8.
- 543 39. **Shen, G. H., B. D. Wu, S. T. Hu, C. F. Lin, K. M. Wu, and J. H. Chen.** 2010. High efficacy of
544 clofazimine and its synergistic effect with amikacin against rapidly growing mycobacteria. *Int J*
545 *Antimicrob Agents* **35**:400-4.
- 546 40. **Phennicie, R. T., M. J. Sullivan, J. T. Singer, J. A. Yoder, and C. H. Kim.** 2010. Specific resistance
547 to *Pseudomonas aeruginosa* infection in zebrafish is mediated by the cystic fibrosis
548 transmembrane conductance regulator. *Infect Immun* **78**:4542-50.
- 549 41. **Bastian, S., N. Veziris, A. L. Roux, F. Brossier, J. L. Gaillard, V. Jarlier, and E. Cambau.** 2011.
550 Assessment of clarithromycin susceptibility in strains belonging to the *Mycobacterium abscessus*
551 group by *erm*(41) and *rrl* sequencing. *Antimicrob Agents Chemother* **55**:775-81.
- 552 42. **Kim, H. Y., B. J. Kim, Y. Kook, Y. J. Yun, J. H. Shin, B. J. Kim, and Y. H. Kook.** 2010.
553 *Mycobacterium massiliense* is differentiated from *Mycobacterium abscessus* and
554 *Mycobacterium bolletii* by erythromycin ribosome methyltransferase gene (*erm*) and
555 clarithromycin susceptibility patterns. *Microbiol Immunol* **54**:347-53.
- 556 43. **Carvalho, R., J. de Sonnevile, O. W. Stockhammer, N. D. Savage, W. J. Veneman, T. H.**
557 **Ottenhoff, R. P. Dirks, A. H. Meijer, and H. P. Spaink.** 2011. A high-throughput screen for
558 tuberculosis progression. *PLoS One* **6**:e16779.

559 44. **Spaink, H. P., C. Cui, M. I. Wiweger, H. J. Jansen, W. J. Veneman, R. Marin-Juez, J. de**
560 **Sonneville, A. Ordas, V. Torraca, W. van der Ent, W. P. Leenders, A. H. Meijer, B. E. Snaar-**
561 **Jagalska, and R. P. Dirks.** 2013. Robotic injection of zebrafish embryos for high-throughput
562 screening in disease models. *Methods* **62**:246-54.
563
564

FIGURE LEGENDS

Figure 1. Kinetics of colonization of *M. abscessus* in aerosolised or intravenously infected BALB/c mice. (A) Mice were aerosolized by 4×10^7 CFU/ml of *Mabs*. Animals were then sacrificed at days 1, 3, 8, 27 prior to CFU counting in the liver, spleen and lungs. Results are expressed as the log units of CFU. **(B)** Mice were challenged *i.v.* 10^6 CFU of *Mabs*. Animals were then sacrificed at days 1, 15 and 30 to determine the CFU counts in the different organs. Results are representative of 2-3 independent experiments and Log CFU are expressed as the mean \pm standard error (n=5-7 mice for each time point).

Figure 2. Experimental protocol to assess the *in vivo* drug activity on *M. abscessus* infection. ZF embryos were *i.v.* infected with ≈ 300 CFU of *Mabs* expressing dtTomato and distributed and incubated into 96-wells plate (1). From 1dpi, embryos were exposed to the drugs of interest which were directly added to the wells. Drugs are then removed and daily renewed for 5 days (2). To determinate the *in vivo* antibacterial effects of the drugs, the embryo survival, the bacterial loads and the evolution of the infection process were monitored at a spatiotemporal level by videomicroscopy (3).

Figure 3. *In vivo* characterization of clarithromycin activity on *M. abscessus* infection. (A-F) Embryos were soaked in clarithromycin at 1.7X, MIC 17X or 170X the MIC for 5 days. The red bar indicates the start and duration of treatment. **(A)** Survival of uninfected embryos treated with various doses of clarithromycin and compared to mock controls (DMSO 1%) (n=20 for each, representative of three independent experiments). Representative microscopy image of an untreated (inset, upper panel) or drug treated-embryo (inset, lower panel) at 8dpf. Clarithromycin appears toxic at the highest concentration as evidenced by the presence

development abnormalities and the increased mortality rate in the drug-exposed embryos compared to the mock control ($p=0.028$, log-rank test). **(B)** Survival of infected *Mabs* treated at various doses of clarithromycin and compared to untreated infected embryos (≈ 300 CFU, $n=20$, representative of three independent experiments). A significant increased survival was observed in the infected-embryos exposed to the highest drug concentration ($p=0.029$, log-rank test). **(C)** Bacterial loads of untreated or treated-embryos (≈ 400 CFU). Results are expressed as mean Log_{10} CFU per embryo from three independent experiments. A significant reduction in bacterial burdens with 170X the MIC in drug treated-embryos is observed at 5dpi. **(D)** Spatiotemporal visualization of the infection by *Mabs* expressing dtTomato (≈ 300 CFU) in untreated or drug treated-embryos. The representative fluorescence and transmission overlay of whole embryos are shown. The yolk is auto-fluorescent. **(E)** Frequency of abscesses in whole untreated or drug treated-embryos over 13dpi (≈ 300 CFU; average of three independent experiments). Infected embryos developed significantly less abscesses in the presence clarithromycin at 170X the MIC than untreated infected-embryos. **(F)** Average localization of abscesses of the infected embryos in (E). *Mabs*-infected ZF developed significantly less abscesses within the brain and the spinal when exposed to the highest clarithromycin dose as compared to untreated infected-ZF. For (c) statistics were calculated using one-way ANOVA or for (e) and (f) with Fisher's exact test comparing each category of drug-treated embryos to untreated control. Error bars represent the standard errors. $**p<0.01$.

Figure 4. Imipenem treatment cures *M. abscessus*-infected embryos. (A-E) From 1dpi, embryos were exposed for 5 days to imipenem concentrations corresponding to 0.5X, 5X or 28X the MIC. **(A)** Survival of infected *Mabs* R treated at various doses of imipenem and compared to untreated infected embryos (≈ 300 CFU, $n=20$, representative of three independent

experiments). Survival of treated R-infected embryos is dose-dependent. Significant increased survival was observed in infected-embryos exposed to 5 X and 28X MIC of imipenem. The red bar indicates the start and duration of treatment. **(B)** Bacterial loads of untreated or imipenem treated-embryos (≈ 400 CFU). Results are expressed as mean Log_{10} CFU per embryo from three independent experiments. A significant decreased of bacterial loads is already observed after 3dpi in the 28X MIC imipenem treated-embryos. **(C)** Spatiotemporal visualization of the infection by *Mabs* expressing dtTomato (≈ 300 CFU) in untreated or imipenem treated-embryos. The representative fluorescence and transmission overlay of whole embryos are shown. **(D)** Frequency of abscesses in whole untreated or imipenem-treated embryos over 13dpi (≈ 300 CFU, average of three independent experiments). Only the 28X MIC imipenem treated-embryos developed significantly fewer abscesses than untreated infected-embryos. **(E)** Average localization of abscesses of the infected embryos in (D). 5X and 28X MIC of imipenem treated-embryos infected by *Mabs* developed fewer abscesses within the brain than untreated infected-embryos. For (B) statistics were calculated using one-way ANOVA or for (D) and (E) with Fisher's exact test comparing each category of imipenem-treated embryos to untreated control. Error bars represent the standard error. * $p=0.02$, ** $p<0.01$, *** $p<0.001$.

Figure 5. Imipenem treatment decreases the early pathophysiological signs within the CNS.

(A-D). dtTomato-expressing *Mabs* (≈ 300 CFU) are injected in 30hpf embryos ($n=15$, average of three independent experiments). From 1dpi, embryos were exposed to imipenem at 0.5X, 5X or 28X MIC during 5 days. **(A)** Fluorescence microscopy of a typical R serpentine cord. Scale bar, 100 μm . **(B)** Fluorescence and DIC overlay of whole heads of a 28X MIC imipenem-treated and untreated infected embryos with red fluorescent *M. abs* showing serpentine cord (white arrow). Scale bars, 100 μm . **(C)** Percentage of embryos with cords in whole untreated and

638 imipenem-treated embryos at 4dpi. A significant reduction in the proportion of embryos with
639 cords was observed when embryos were treated with the highest (28X MIC) imipenem
640 concentration. **(D)** Average localization of cord of the infected embryos in (C). Infected embryos
641 treated with the intermediate (5X MIC) and high (28X MIC) imipenem doses developed
642 significantly fewer serpentine cords within the CNS compared to untreated infected-embryos.
643 For (C) and (D), statistics were calculated using Fisher's exact test comparing each category of
644 imipenem-treated embryos to untreated control. All results are expressed as the average from
645 three independent experiments and error bars represent the standard errors.

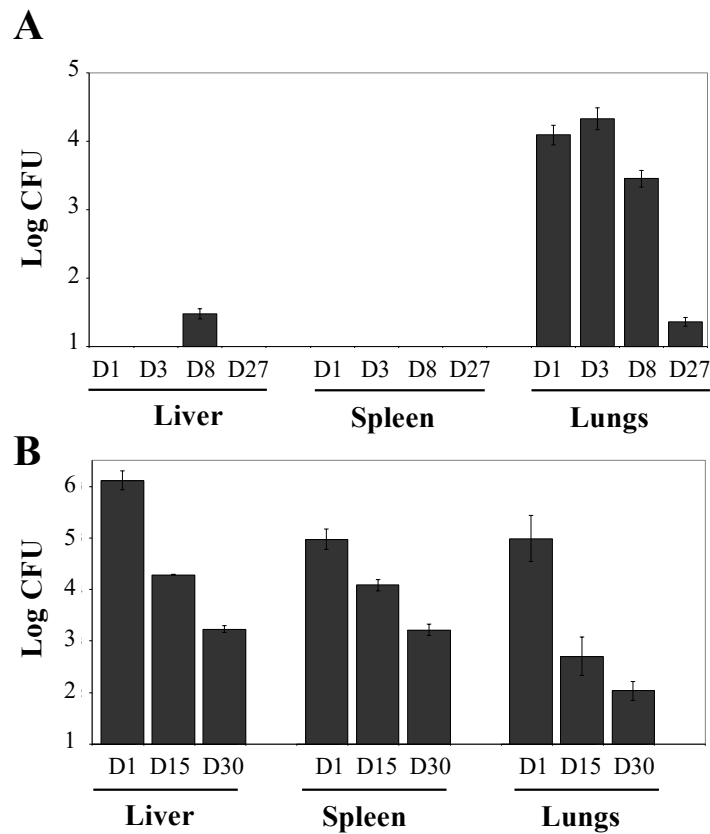


Figure 1. Kinetics of colonization of *M. abscessus* in aerosolised or intravenously infected BALB/c mice. **(A)** Mice were aerosolized by 4×10^7 CFU/ml of *Mabs*. Animals were then sacrificed at days 1, 3, 8, 27 prior to CFU counting in the liver, spleen and lungs. Results are expressed as the log units of CFU. **(B)** Mice were challenged *i.v.* 10^6 CFU of *Mabs*. Animals were then sacrificed at days 1, 15 and 30 to determine the CFU counts in the different organs. Results are representative of 2-3 independent experiments and Log CFU are expressed as the mean \pm standard error (n=5-7 mice for each time point).

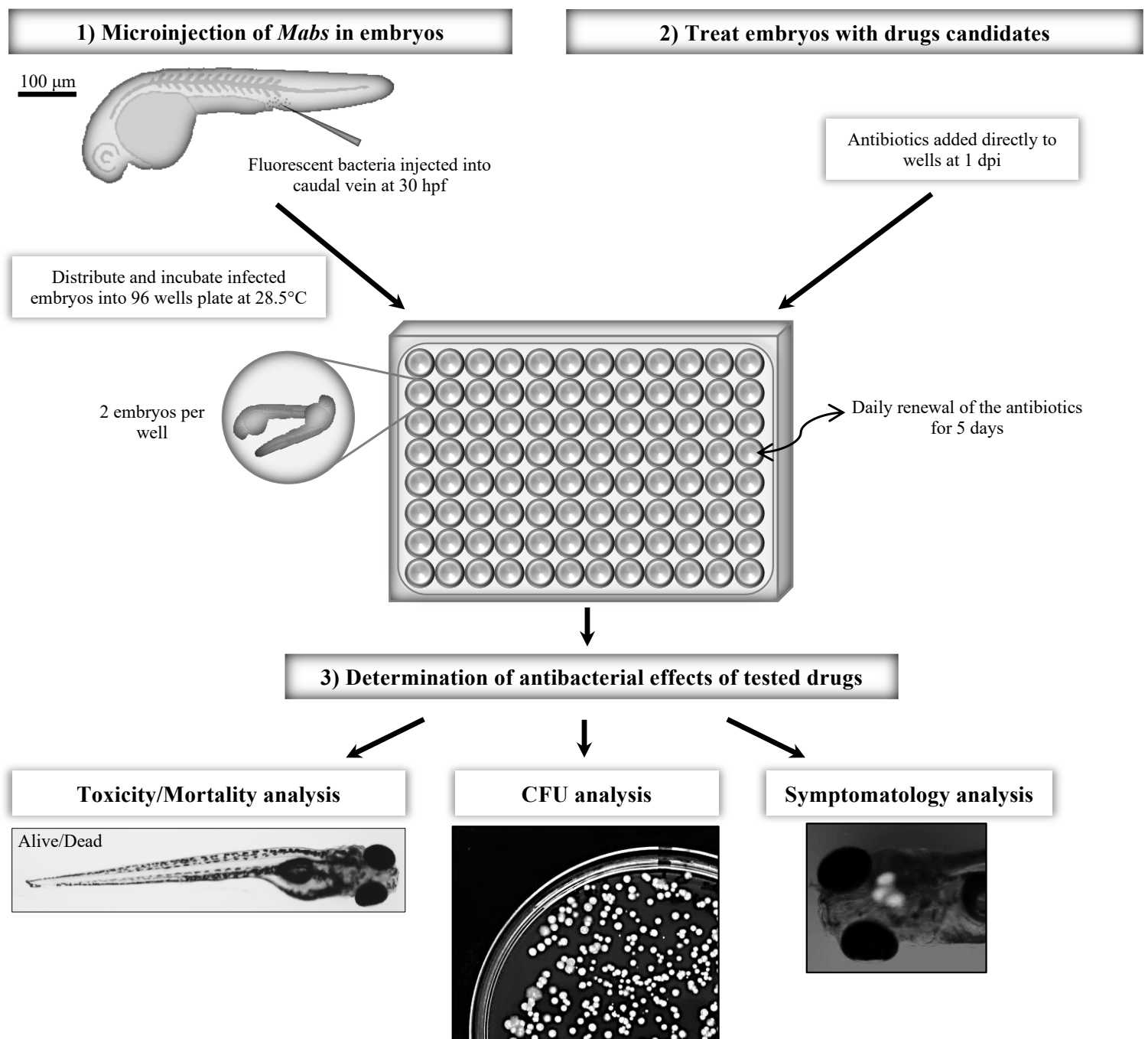


Figure 2. Experimental protocol to assess the *in vivo* drug activity on *M. abscessus* infection. ZF embryos were *i.v.* infected with ≈ 300 CFU of *Mabs* expressing dtTomato and distributed and incubated into 96-wells plate (1). From 1dpi, embryos were exposed to the drugs of interest which were directly added to the wells. Drugs are then removed and daily renewed for 5 days (2). To determinate the *in vivo* antibacterial effects of the drugs, the embryo survival, the bacterial loads and the evolution of the infection process were monitored at a spatiotemporal level by videomicroscopy (3).

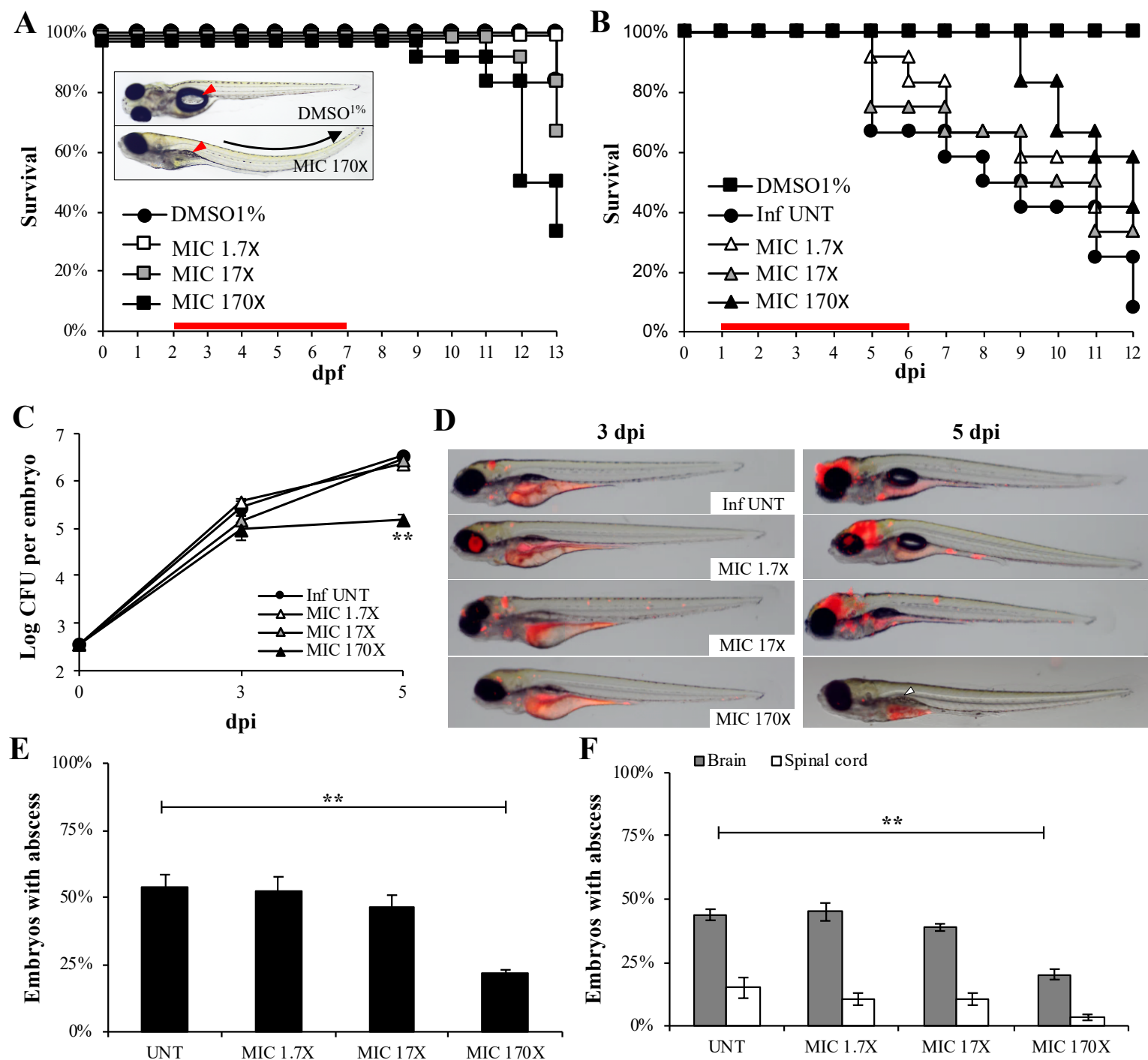


Figure 3. *In vivo* characterization of clarithromycin activity on *M. abscessus* infection. (A-F) Embryos were soaked in clarithromycin at 1.7X, MIC 17X or 170X the MIC for 5 days. The red bar indicates the start and duration of treatment. **(A)** Survival of uninfected embryos treated with various doses of clarithromycin and compared to mock controls (DMSO 1%) (n=20 for each, representative of three independent experiments). Representative microscopy image of an untreated (inset, upper panel) or drug-treated-embryo (inset, lower panel) at 8dpf. Clarithromycin appears toxic at the highest concentration as evidenced by the presence of development abnormalities and the increased mortality rate in the drug-exposed embryos compared to the mock control (p=0.028, log-rank test). **(B)** Survival of infected *Mabs* treated at various doses of clarithromycin and compared to untreated infected embryos (≈300 CFU, n=20, representative of three independent experiments). A significant increased survival was observed in the infected-embryos exposed to the highest drug concentration (p=0.029, log-rank test). **(C)** Bacterial loads of untreated or treated-embryos (≈400 CFU). Results are expressed as mean Log₁₀ CFU per embryo from three independent experiments. A significant reduction in bacterial burdens with 170X the MIC in drug-treated-embryos is observed at 5dpi (**). **(D)** Spatiotemporal visualization of the infection by *Mabs* expressing dtTomato (≈300 CFU) in untreated or drug-treated-embryos. The representative fluorescence and transmission overlay of whole embryos are shown. The yolk is auto-fluorescent. **(E)** Frequency of abscesses in whole untreated or drug-treated-embryos over 13dpi (≈300 CFU; average of three independent experiments). Infected embryos developed significantly less abscesses in the presence of clarithromycin at 170X the MIC than untreated infected-embryos (**). **(F)** Average localization of abscesses of the infected embryos in (E). *Mabs*-infected ZF developed significantly less abscesses within the brain and the spinal cord when exposed to the highest clarithromycin dose as compared to untreated infected-ZF. For (c) statistics were calculated using one-way ANOVA or for (e) and (f) with Fisher's exact test comparing each category of drug-treated embryos to untreated control. Error bars represent the standard errors. **p<0.01.

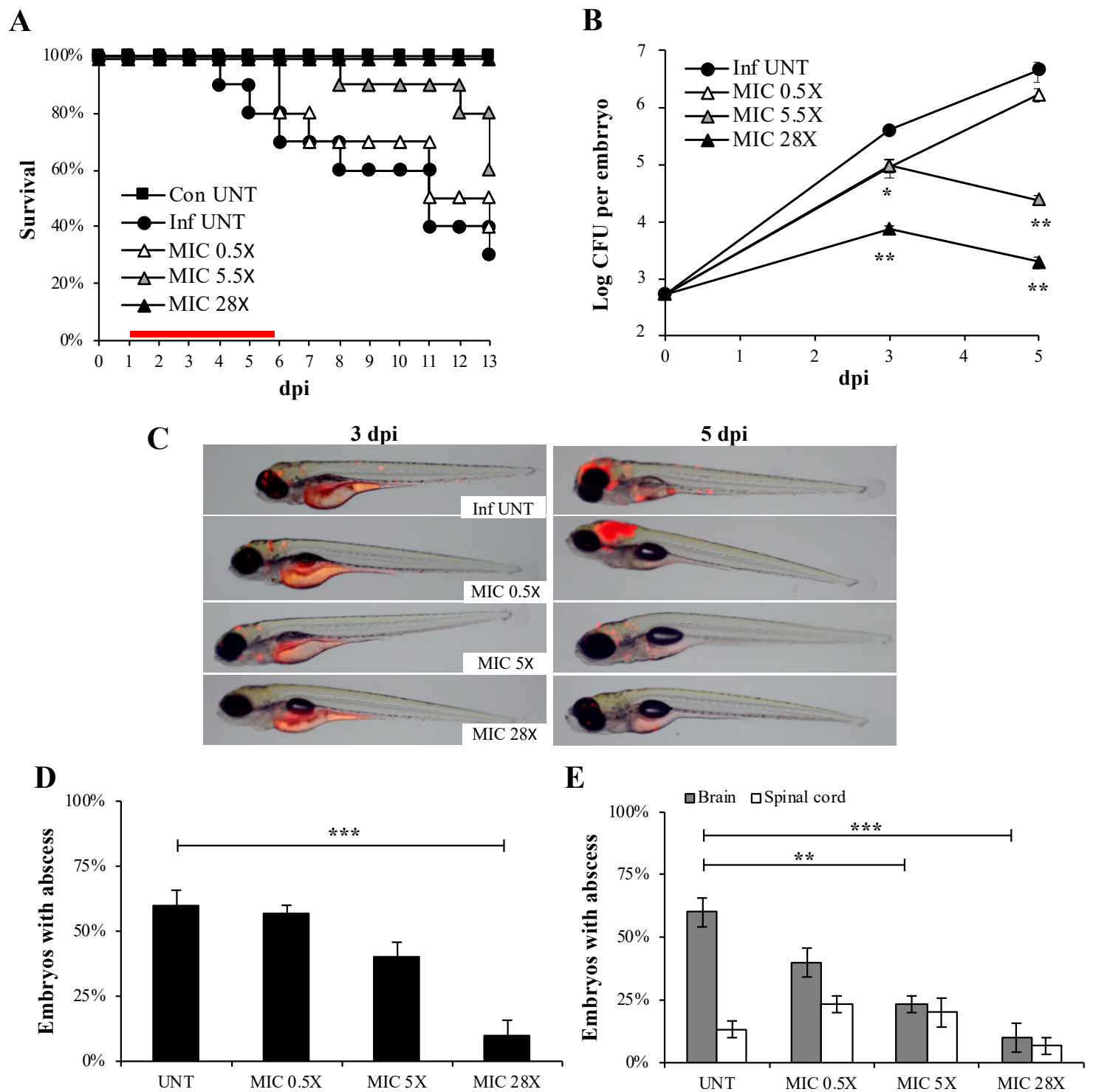


Figure 4. Imipenem treatment cures *M. abscessus*-infected embryos. (A-E) From 1dpi, embryos were exposed for 5 days to imipenem concentrations corresponding to 0.5X, 5X or 28X the MIC. **(A)** Survival of infected *Mabs* R treated at various doses of imipenem and compared to untreated infected embryos (≈ 300 CFU, $n=20$, representative of three independent experiments). Survival of treated R-infected embryos is dose-dependent. Significant increased survival was observed in infected-embryos exposed to 5 X and 28X MIC of imipenem. The red bar indicates the start and duration of treatment. **(B)** Bacterial loads of untreated or imipenem treated-embryos (≈ 400 CFU). Results are expressed as mean Log_{10} CFU per embryo from three independent experiments. A significant decreased of bacterial loads is already observed after 3dpi in the 28X MIC imipenem treated-embryos. **(C)** Spatiotemporal visualization of the infection by *Mabs* expressing dtTomato (≈ 300 CFU) in untreated or imipenem treated-embryos. The representative fluorescence and transmission overlay of whole embryos are shown. **(D)** Frequency of abscesses in whole untreated or imipenem-treated embryos over 13dpi (≈ 300 CFU, average of three independent experiments). Only the 28X MIC imipenem treated-embryos developed significantly fewer abscesses than untreated infected-embryos. **(E)** Average localization of abscesses of the infected embryos in (D). 5X and 28X MIC of imipenem treated-embryos infected by *Mabs* developed fewer abscesses within the brain than untreated infected-embryos. For (B) statistics were calculated using one-way ANOVA or for (D) and (E) with Fisher's exact test comparing each category of imipenem-treated embryos to untreated control. Error bars represent the standard error. * $p=0.02$, ** $p<0.01$, *** $p<0.001$.

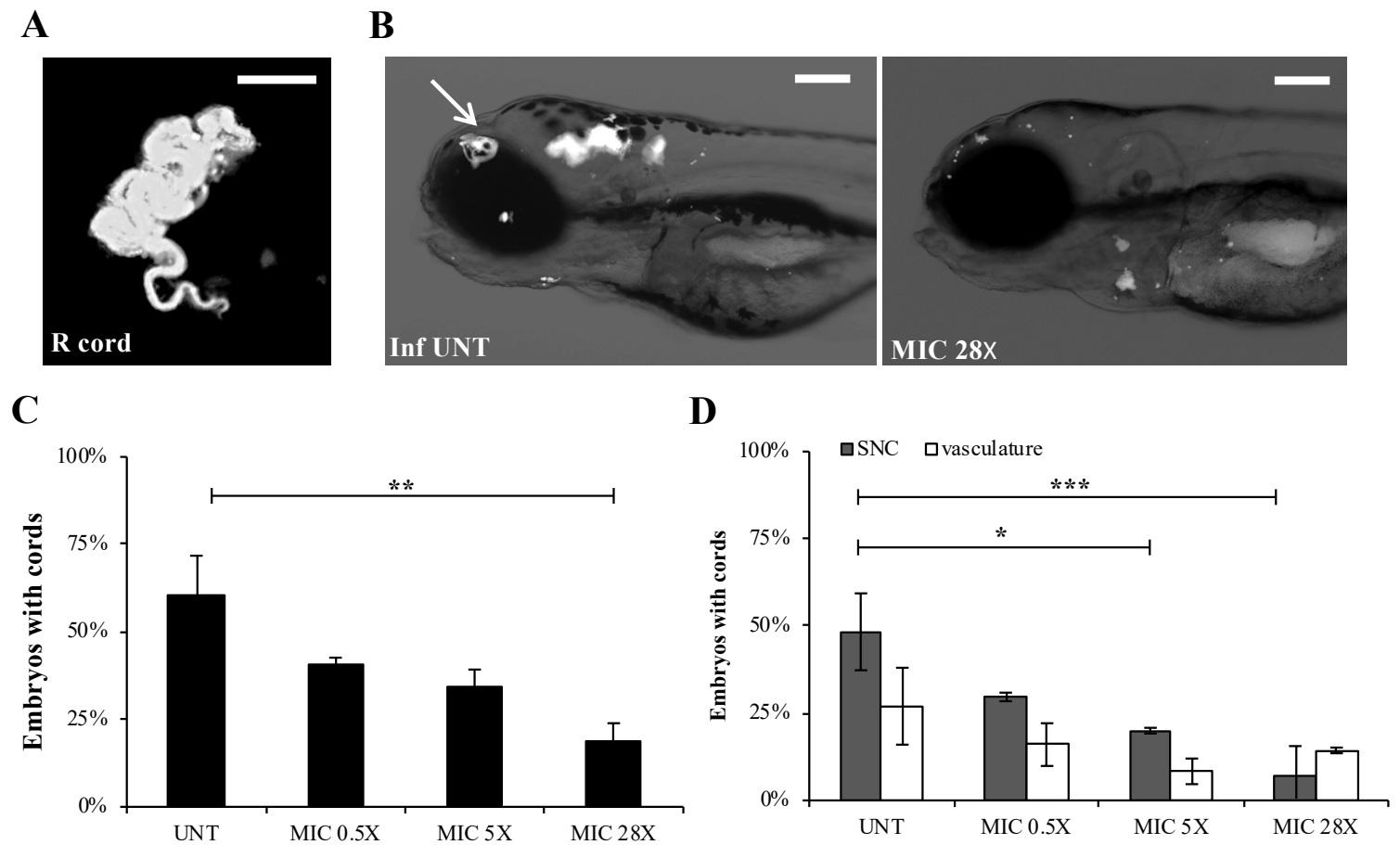


Figure 5. Imipenem treatment decreases the early pathophysiological signs within the CNS. (A-D). dtTomato-expressing *Mabs* (≈ 300 CFU) are injected in 30hpf embryos ($n=15$, average of three independent experiments). From 1dpi, embryos were exposed to imipenem at 0.5X, 5X or 28X MIC during 5 days. **(A)** Fluorescence microscopy of a typical R serpentine cord. Scale bar, $100\mu\text{m}$. **(B)** Fluorescence and DIC overlay of whole heads of a 28X MIC imipenem-treated and untreated infected embryos with red fluorescent *M. abs* showing serpentine cord (white arrow). Scale bars, $100\mu\text{m}$. **(C)** Percentage of embryos with cords in whole untreated and imipenem-treated embryos at 4dpi. A significant reduction in the proportion of embryos with cords was observed when embryos were treated with the highest (28X MIC) imipenem concentration. **(D)** Average localization of cord of the infected embryos in (C). Infected embryos treated with the intermediate (5X MIC) and high (28X MIC) imipenem doses developed significantly fewer serpentine cords within the CNS compared to untreated infected-embryos. For (C) and (D), statistics were calculated using Fisher's exact test comparing each category of imipenem-treated embryos to untreated control. All results are expressed as the average from three independent experiments and error bars represent the standard errors.

SUPPLEMENTAL MATERIAL

***In vivo* assessment of drug efficacy against *Mycobacterium abscessus* using the embryonic zebrafish test system**

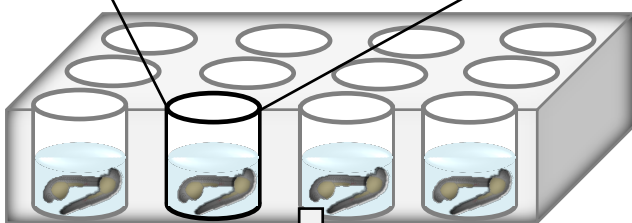
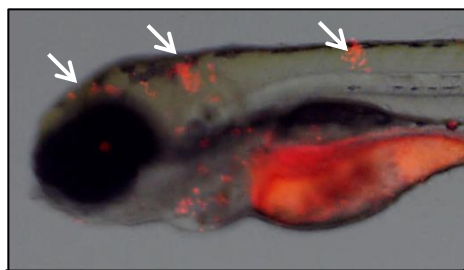
Audrey Bernut¹, Vincent Le Moigne³, Tiffany Lesne¹, Georges Lutfalla¹,
Jean-Louis Herrmann³ and Laurent Kremer^{1,2,#}

A

Microinjection of fluorescent bacteria
into caudal vein at 30hpf



Incubate infected embryos
for 3 days at 28.5 °C



Add imipenem into wells
Daily drug renewal for 5 days



Drug activity assessment
(monitoring survival and
abscess evolution)

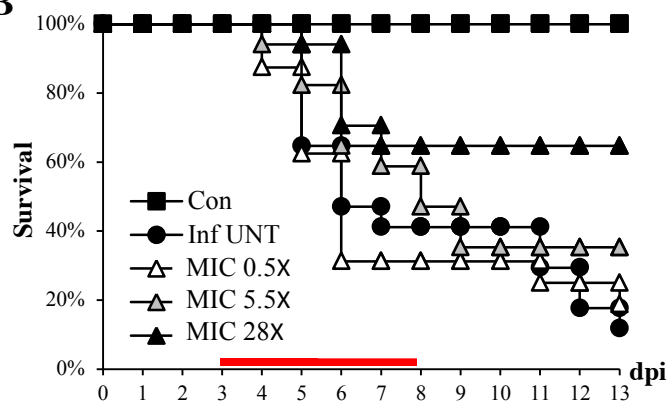
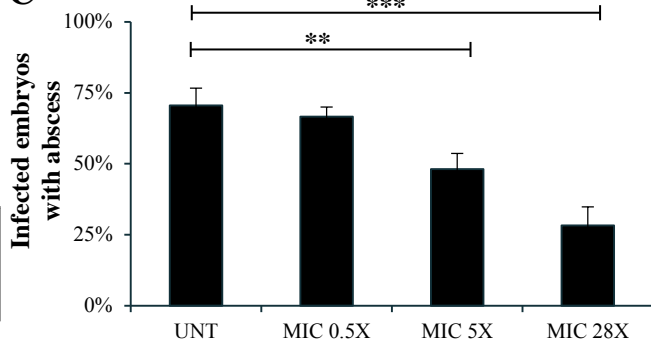
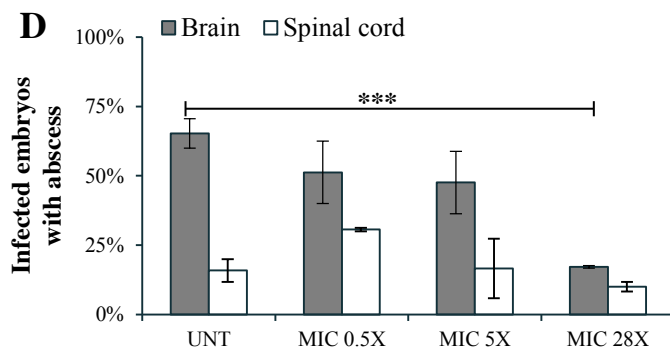
B**C****D**

Figure S1. Exposure to imipenem overcomes and protects against severe *M. abscessus* infections. (A-C) dtTomato expressing *Mabs* (≈ 300 CFU) were injected in 30hpf embryos. From 3dpi, embryos were exposed during 5 days to imipenem at 0.5X, 5X or 28X MIC. (A) Schematic representation illustrating the “curing” protocol used as well as the infection status of the embryos at 3dpi (numerous abscesses within the CNS) when the drug treatment is applied. (B) Survival of infected *Mabs* treated at various doses of imipenem and compared to untreated infected embryos ($n=20-30$), representative of three independent experiments). A significant increased survival was observed in embryos exposed to the highest (28X MIC) imipenem dose. The red bar indicates the start and duration of treatment. (C) Frequency of *Mabs* abscesses in whole untreated or imipenem-treated embryos over 13dpi. Data are expressed as the average of three independent experiments. MIC 5X and MIC 28X imipenem treated-embryos infected by *Mabs* developed significantly fewer abscesses than untreated infected-embryos. (D) Average localization of abscesses of the infected embryos in (C). 28X MIC imipenem treated-embryos infected by *Mabs* developed significantly fewer abscesses within the brain than untreated infected-embryos. For (C) and (D) statistics were calculated using Fisher’s exact test comparing each category of imipenem-treated embryos to untreated control. All results are expressed as the average from two or three independent experiments and error bars represent the standard errors. ** $p<0.01$, *** $p<0.001$.

Table S1. Minimal inhibitory concentrations of several drugs against *M. abscessus* using the microdilution method in cation-adjusted Mueller-Hinton (MH) broth or on LB agar. Antibiotics used in infected ZF are shown in bold. Results are expressed in μM and $\mu\text{g/ml}$.

Antibiotic	Molecular weight	Solvent	MIC MH broth		MIC LB agar	
			μM	$\mu\text{g/mL}$	μM	$\mu\text{g/mL}$
Clarithromycin	748	DMSO	4	3.0	0.7	0.5
Cefoxitin	427	DMSO	60	25.6	35	15
Amikacin	586	H ₂ O	125	73.25	26	15
Isoniazid	137	H ₂ O	1000	137	365	50
Erythromycin	734	DMSO	125	91.75	10	7.5
Imipenem	299	H₂O	60	17.94	3.3	1
Thiacetazone	236	DMSO	1000	236	42	10